NeuroImage 167 (2018) 53–61

Contents lists available at ScienceDirect

NeuroImage

journal homepage: www.elsevier.com/locate/neuroimage

Analyzing EEG and MEG signals recorded during tES, a reply

Nima Noury [a,b,*], Markus Siegel [a,**]

[a] Centre for Integrative Neuroscience & MEG Center, University of Tübingen, Germany
[b] IMPRS for Cognitive and Systems Neuroscience, Tübingen, Germany

ARTICLE INFO

Keywords:
Transcranial electric stimulation (tES)
Transcranial alternating current stimulation (tACS)
Transcranial direct current stimulation (tDCS)
EEG
MEG
Neural entrainment
Stimulation artifacts

ABSTRACT

Transcranial Electric Stimulation (tES) is a widely used non-invasive brain stimulation technique. However, strong stimulation artifacts complicate the investigation of neural activity with EEG or MEG during tES. Thus, studying brain signals during tES requires detailed knowledge about the properties of these artifacts. Recently, we characterized the phase- and amplitude-relationship between tES stimulation currents and tES artifacts in EEG and MEG and provided a mathematical model of these artifacts (Noury and Siegel, 2017, and Noury et al., 2016, respectively). Among several other features, we showed that, independent of the stimulation current, the amplitude of tES artifacts is modulated time locked to heartbeat and respiration. In response to our work, a recent paper (Neuling et al., 2017) raised several points concerning the employed stimulation device and methodology. Here, we discuss these points, explain potential misunderstandings, and show that none of the raised concerns are applicable to our results. Furthermore, we explain in detail the physics underlying tES artifacts, and discuss several approaches how to study brain function during tES in the presence of residual artifacts.

1. Introduction

Transcranial Electric Stimulation (tES) is a noninvasive brain stimulation technique that is widely used to manipulate brain function (Fertonani and Miniussi, 2016; Kuo and Nitsche, 2012). However, the neurophysiological mechanisms underlying tES effects are largely unknown, mainly because strong stimulation artifacts render the electrophysiological investigation of brain activity with EEG or MEG during tES challenging (Bergmann et al., 2016; Thut et al., 2017). Such simultaneous measurements may not only provide insights into the mechanisms underlying tES effects, but may also pave the way for new feedback-controlled brain stimulation protocols, in which stimulation parameters are continuously optimized based on the simultaneously recorded brain activity (Bergmann et al., 2016; Brittain et al., 2013; Lustenberger et al., 2016; Romei et al., 2016).

Despite several efforts to remove tES artifacts from simultaneously recorded EEG and MEG signals, a comprehensive artifact-removal pipeline that completely removes artifacts is still missing (Helfrich et al., 2014; Neuling et al., 2015; Soekadar et al., 2013; Voss et al., 2014). This is at least partly because the employed methods have been designed and used without considering the properties of tES artifacts. Recently, we characterized both, amplitude (Noury et al., 2016) and phase (Noury and Siegel, 2017) properties of tES artifacts for EEG and MEG. We suggested a mathematical model for the transfer function that defines the relationship between the stimulation current and tES artifacts and may be used for simulating tES artifacts (Noury and Siegel, 2017). We showed that the mapping between stimulation current and tES artifacts is non-linear and time-varying. The non-linearity manifests itself in the amplitude and phase of stimulation artifacts. Moreover, both, phase and amplitude of artifacts are rhythmically modulated time-locked to heartbeats and respiration, due to body resistance changes and head movements. These modulations have a time-varying spatial pattern, which makes the transfer function time-varying. We used the rhythmic modulation of artifact amplitudes as landmarks of tES artifacts to quantify their bandwidth in the frequency domain, and to detect the presence of artifacts at different stages of available artifact-removal pipelines. We showed that none of the available artifact-removal pipelines is able to completely remove stimulation artifacts. Therefore, we concluded that residual artifacts need to be considered to prevent false positive results and wrong conclusions (Noury et al., 2016).

In response to our work regarding the amplitude of tES artifacts (Noury et al., 2016), a recent paper (Neuling et al., 2017) raised several concerns. First, Neuling et al. argued that the amplitude modulations reported by us were due to a malfunction of our stimulation device.

* Corresponding author. Centre for Integrative Neuroscience, University of Tübingen, Otfried-Müller-Str. 25, 72076 Tübingen, Germany.
** Corresponding author. Centre for Integrative Neuroscience, University of Tübingen, Otfried-Müller-Str. 25, 72076 Tübingen, Germany.
E-mail addresses: nima.noury@cin.uni-tuebingen.de (N. Noury), markus.siegel@uni-tuebingen.de (M. Siegel).

https://doi.org/10.1016/j.neuroimage.2017.11.023
Received 15 August 2017; Accepted 12 November 2017
Available online 14 November 2017

Second, they suggested that wrong parameters in our beamforming pipeline led to residual artifacts in our source-level estimations. We suspect that these concerns may be based on a misunderstanding of our results and of the physics underlying tES artifacts, because several findings in our previous paper ruled out the raised concerns, and because the authors made both their claims without applying the critical analyses suggested in our paper to their data. Therefore, in section 3, we first discuss in detail the physics behind amplitude modulations of tES artifacts, explain our previous findings in more detail, and suggest methods to detect artifacts in raw and processed signals (Table 1). In section 4, we then systematically discuss all sections of Neuling et al. (2017) and show that none of the raised concerns are correct or relevant to our results. Finally, in section 5, we point out several approaches and directions on how brain signals recorded during tES can be studied (Table 1).

2. Materials and methods

Most of the materials and methods have been described in detail before (Noury et al., 2016; Noury and Siegel, 2017). Thus, here we focus only on new materials and methods.

2.1. Participants and data acquisition

All experiments were conducted in 3 healthy male participants. Two of the subjects participated in a transcranial alternating current stimulation (tACS) experiment with three stimulation conditions: sham, 11 Hz, and 62 Hz tACS. Stimulation currents of 1 mA peak-to-peak were applied with an IZ2h stimulator (Tucker Davis Technologies Inc.), either through large rubber electrodes (35 cm^2 MR-compatible, neuroConn GmbH), or small Ag/AgCl EEG electrodes. Stimulation electrodes' impedance was kept below 2.5 kΩ. We simultaneously recorded the EEG (NeurOne system, Mega Electronics Ltd), MEG (Omega 2000, CTF Systems), injected current, ECG and respiratory movements during the tACS experiments. The injected current was indirectly measured by recording the voltage drop across a 200 Ω resistor positioned in series to the head.

In another experiment, a third subject's head movement during an MEG experiment was continuously measured for 10 min during fixation at rest. The head position relative to the MEG sensors was measured using three head localization coils (nasion, left/right preauricular points; sampling rate: 24.4 Hz). The MEG's localization coil movement data were converted to head movements using the method presented in Stolk et al. (2013). The subject's ECG was recorded simultaneously.

2.2. Data analyses

To remove an optimal sinusoidal model from artifactual signals, we fitted the amplitude, frequency and phase of a sinusoid to the MEG and EEG data and subtracted it from the data.

High-resolution power spectral density (PSD) of EEG and MEG signals was estimated on Hanning-windowed 33 s or 5 s data segments. In a similar manner, PSD of the mean-removed head movement was calculated using 30 s segments. For simulating the effect of amplitude modulation using head movement signal, we multiplied the normalized head movement signal (x axis) with a sinusoid of amplitude one. As the sampling rate of the MEG was not an integer number, signal segments were not exactly 30 s long. Thus, to avoid power leakage of the main peak to nearby frequencies, we set the sinusoid's frequency equal to the sampled FFT frequency that was closest to 11 Hz.

We applied adaptive linear spatial filtering (beamforming) (Van Veen et al., 1997) to the MEG data of the experiment with small stimulation electrodes and 11 Hz tACS. The procedure was exactly as explained in Noury et al. (2016). Importantly, during application of tACS the high signal power caused by the stimulation artifact makes it difficult to determine the cutoff between brain signals and sensor noise. Thus, we set the regularization factor (λ), which is an estimate of measurement noise, based on sham recordings only. To this end, we applied PCA on the sham recordings, and set the regularization factor equal to the Eigenvalue of the PC at which the cumulative explained variance reached 99% of the total variance.

To check the effect of the regularization factor on the beamforming results (Fig. 4), we also estimated source level activity using λ values of 0%, 1e-7%, 5%, 15%, 100%, 300% and 600%. These values were defined as percentages relative to the average power of MEG sensor-level signals during pooled sham and tACS conditions.

All data analyses were performed in Matlab (MathWorks) using custom scripts and the open source toolbox Fieldtrip (Oostenveld et al., 2011).

3. tES artifacts

In this section, we first explain the physics underlying tES artifacts, and then discuss methods and obstacles of detecting artifacts in EEG and MEG (Table 1).

3.1. Physics underlying amplitude modulations of tES artifacts

EEG measures the voltage difference between a reference electrode and electrodes placed at different points on the head as defined by Ohm's law:

$$\Delta V = -\int \rho\, J.dl \tag{1}$$

$$\Delta V_{eeg} = \alpha.\ \Delta V$$

Considering tES artifacts, ΔV stands for the voltage difference between two points on the body, ΔV_{eeg} is the voltage that the EEG device reports, α is a scale factor (close to one) that depends on electrode impedances, which may induce phase-shifts through capacitive effects, and on the input resistance of the EEG amplifier, J is the stimulation current density vector on the head (in A/m^2), ρ is the head's electrical resistivity (in Ω.m), dl is a path element, and the integral is along the path from the skin underlying the reference EEG electrode to the skin underlying a specific EEG electrode.

MEG, on the other hand, measures the magnetic fields generated by current sources mainly inside the MEG room. Under the quasi-static condition (Baillet et al., 2001), the magnetic field is defined by the Biot-Savart law:

$$B = \frac{\mu}{4\pi}\iiint_{v}\frac{(J\,dV)\times r'}{|r'|^3} \tag{2}$$

For the case of tES artifacts, B is the artifactual magnetic field sensed by an MEG sensor, J is the stimulation current density vector in stimulation wires, stimulation electrodes, and on the head, r' is the distance vector between the position of the electrical current and the MEG sensor, μ is the magnetic permeability, and dV is the volume element. It is worth noting that recent findings indicate small phase shifts of tACS artifacts relative to the stimulation current, which may be due to the influence of time-varying electromagnetic waves produced by tACS currents (see Noury and Siegel, 2017 for more information on phase features of tES artifacts). In other words, the quasi-static estimation of magnetic fields during tACS (i.e. equation (2)) may not reflect all aspects of the stimulation artifacts. However, the influence of such time-varying electromagnetic fields should be small, and thus, equation (2) can be used to explain the basic features of the stimulation artifact's amplitude.

From equations (1) and (2), it follows that the stimulation current linearly scales tES artifacts. Therefore, to identify the origin of any observed electromagnetic effect during tES, it is necessary to first closely examine the waveform of the injected current. In other words, one must make sure that the observed effects do not already exist in the output current of the stimulation device. In particular, it is necessary to rule out wrong conclusions resulting from a malfunction of the stimulation device

(Noury et al., 2016). The stimulation current can be measured by recording the voltage drop across a small resistance positioned in series to the head by means of an EEG amplifier. Importantly, this resistance needs to be small enough that the produced voltage drop does not exceed the dynamic range of the EEG device.

TES artifacts would only reflect a scaled version of the injected current, i.e. a linear and time-invariant transformation, if except from the stimulation current no other part of equations (1) and (2) was time varying. However, the EEG electrode impedance, the body's resistivity (ρ) (Fisch, 1999), and head position (r') (Stolk et al., 2013) are all time varying. From equations (1) and (2) it follows that any change in the spatial pattern of the body's resistivity or electrode impedance, and any change in the distance between the stimulation current and the MEG sensors, results in a change of the observed tES artifact for EEG and MEG. In other words, because of the multiplications in equations (1) and (2), changes in α, ρ and r' over time result in modulations of the amplitude of stimulation artifacts. For EEG, this is simply because any change in impedance changes the voltage drop measured by the EEG device. For MEG, moving a current source closer to an MEG sensor increases the magnetic field that is sensed by that MEG sensor. It is worth noting that, as the stimulation current (J) is orders of magnitude bigger than normal physiological currents, the multiplications in (1) and (2) have magnifying effects such that even very small changes of α, ρ and r' can lead to tES artifact modulations comparable to the strength of physiological signals of interest at the sensor level.

The above-mentioned amplitude modulation (AM) of stimulation artifacts in the time domain has a direct influence on the power spectrum of stimulation artifacts in the frequency domain. Because multiplication in the time domain translates to convolution in the frequency domain (Oppenheim and Schafer, 2009), amplitude modulation of artifacts, in the frequency domain leads to artifacts with symmetric power spectra and a wider bandwidth compared to the bandwidth of the injected current. In case of a stimulation current with a sharp main peak at f_{stim} and a modulation waveform with bandwidth W, the resulting tES artifact will have a bandwidth of $2W$ (i.e. the frequency band from $f_{stim} - W$ to $f_{stim} + W$), and a symmetric power spectrum that contains normal and mirrored versions of the spectrum of the modulation waveform around the main stimulation peak (Fig. 1). For the special case of tDCS, the artifact will occupy the frequency band from 0 to W.

Apart from the symmetricity of tES artifacts in the frequency domain, the artifacts' power spectra have other general features that derive from properties of the body's resistivity (ρ) and head position (r'). In general, temporal changes in ρ and r' include both slow non-rhythmic components like sweating (for ρ) and head drift (for r'), and rhythmic components like eye blinks (for ρ), heartbeats, and respiration (for both ρ and r', Dornhorst et al., 1952; Kristiansen et al., 2005; Michard, 2005; Nyboer et al., 1950; Pinheiro et al., 2010; Stolk et al., 2013). In the frequency domain, power spectra of these modulations have a general 1/f appearance due to the arrhythmic components, with several local peaks at frequencies of rhythmic variations and/or their harmonics (Fig. 2A). Therefore, as a results of the AM mechanism explained above, artifacts at the sensor level have a symmetric power spectrum that decays at frequencies away from the stimulation frequency, and shows symmetric local side peaks at the stimulation frequency ± the fundamental and harmonic frequencies of rhythmic variations of ρ and r' (Fig. 2B).

It is important to note that both, non-rhythmic and rhythmic components of the artifact amplitude modulation should be removed from the data before attempting to assess brain activity. However, a major problem is that no ground truth is currently available for evaluating the output of artifact cleaning methods. As suggested in Noury et al. (2016), in the absence of ground truth, one possibility is to use the known features of artifacts to test the presence of residual artifacts at different stages of artifact cleaning pipelines. Notably, because of the lack of information about specific features of non-rhythmic artifact modulations, it is particularly difficult to track and dissociate these non-rhythmic artifact modulations from brain activity. Nevertheless, the broadband symmetricity of the spectrum, and peaks related to heartbeat and respiration induced artifact modulations are two critical artifact features that can be used for such tests. Based on these two features, in Noury et al. (2016), we presented several methods for detecting and tracking artifacts in time, frequency and space, which we briefly present in the following.

3.2. Detecting artifacts in raw recordings

Prior to the application of artifact cleaning methods and in each subject, heartbeat and respiration-induced modulations of artifacts can be well detected in the time domain by analyzing each channel's artifact amplitude, time-locked to heartbeats and respiration. Another way is to determine if local peaks of the high-resolution spectrum around the stimulation frequency match the predicted frequencies for artifactual side peaks based on the AM model as explained above. Compared to the time domain analysis, this is a less sensitive method, because it does not use all the information about the timing of heartbeats and respiration. Furthermore, in the frequency domain, several confounds may hinder the detection of rhythmic artifact modulations (Noury et al., 2016). In particular, power leakage of the main stimulation peak, strong non-rhythmic artifact modulations, and overlapping brain activity are three confounds that we briefly explain next.

Table 1
Summary of approaches to detect tES artifacts and to study brain activity in the presence of residual artifacts. See main text for explanations.

General prerequisites
Record stimulation current to rule-out stimulator malfunction
Record ECG, respiration, head movement, body impedance etc. to analyse artifact modulations
Detecting artifacts
Time domain: Modulation of artifact amplitude and phase time-locked to heartbeats and respiration?
Frequency domain: Symmetric side-peaks at the stimulation frequency ± frequency of physiological rhythms? Caveats: Remove sine wave fit to suppress FFT power leakage; Check side-peaks corresponding to harmonics of physiological rhythms to avoid masking by non-rhythmic artifact modulation *Cross-frequency analysis*: Correlation of temporal or spatial patterns of results (e.g. source-level power) between the stimulation frequency and the stimulation frequency ± frequency of physiological rhythms? (particularly suited to detect residual artifacts)
Coping with residual artifacts
Evaluate the strength of residual artifacts using *simulations* or *control experiments*
Event related responses are free of residual artifacts under specific conditions
Contrast two populations with identical residual artifacts (subtract, but not divide)

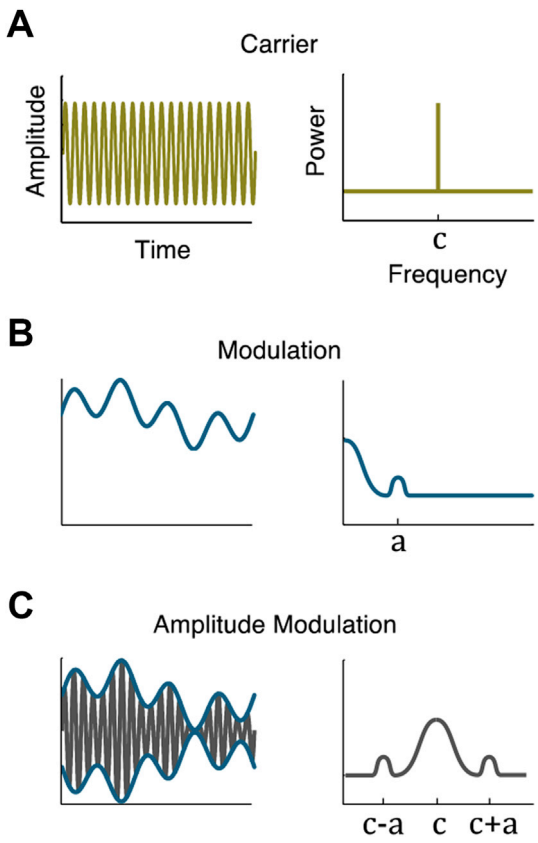

Fig. 1. Schematic illustration of amplitude modulation (AM) in the time (left) and frequency (right) domain. In this example, the carrier signal (A) is a pure sinusoidal wave with constant amplitude. The ideal estimation of the power spectrum of such a signal contains only a sharp peak at the carrier frequency *c*. A modulation wave shows slow variations over time (B left). These variations can be rhythmic or arrhythmic. Rhythmic variations correspond to a peak in the power spectrum at frequency *a*, and non-rhythmic variations correspond to a power increase at low frequencies (B right). Multiplying the carrier signal with the modulation wave, yields the amplitude-modulated signal (C left). Multiplication in the time domain corresponds to convolution in the frequency domain. Therefore, the power spectrum of the amplitude-modulated signal is symmetric, with the power spectrum of the modulation wave and its mirrored version around the carrier frequency.

3.3. Power leakage

If stimulation and recording devices share the same clock, the power spectrum is estimated with high resolution, and the data is segmented properly, the main peak at the stimulation frequency will be sharp and will not leak to nearby frequencies (Fig. 2B). However, normally this is not the case and, even after appropriate windowing, the strong peak at the stimulation frequency leaks to nearby frequencies, which may mask important details of the spectrum. As explained in Noury et al. (2016), to solve this problem and to uncover details of the power spectrum, one needs to first remove a non-linearly fitted sine model of the stimulation artifact from the recorded signal of each channel. This procedure does not only substantially reduce the stimulation peak itself, but also its spectral leakage, which helps to uncover artifact peaks at frequencies close to the stimulation frequency (compare dark gray vs. magenta curves in Fig. 3C–F).

3.4. Non-rhythmic components

As explained above, non-rhythmic components of artifact modulations generate a symmetrical 1/f decay of the power spectrum around the stimulation frequency. In particular close to the stimulation frequency, this may mask artifactual peaks. As this contamination decays away from the stimulation frequency, side peaks related to harmonics of rhythmic modulations may be easier to detect than the side peaks at the fundamental frequency of rhythmic modulations (Fig. 3F).

3.5. Overlapping brain activity

Power spectra of M/EEG during tACS reflect both, brain activity and stimulation artifacts. Therefore, strong brain activity at the stimulation frequency may mask details of the artifact's spectrum and may influence its symmetric appearance (Fig. 3C, F). As the power of brain signals generally decays at higher frequencies, stimulation artifacts at higher frequencies are generally easier to observe (artifacts are easier observable in Fig. 3D, F than in Fig. 3C, E). Therefore, control stimulation conditions at high frequencies (for example in the high gamma range or higher) may be useful for revealing the spectral features of stimulation artifacts.

3.6. Detecting residual artifacts and cross-frequency analysis

The above-mentioned tools for detecting stimulation artifacts prior to application of artifact-cleaning methods may not be able to detect residual artifacts after artifact cleaning. As detailed in Noury et al. (2016), this is mainly due to two reasons. First, artifact-cleaning methods strongly attenuate artifacts. Therefore, brain activity may mask the spectral and temporal landmarks of residual artifacts. Second, artifact-cleaning methods (e.g., template subtraction) may destroy the consistent pattern of rhythmic artifactual modulations.

Importantly, difficulties in detecting the residual artifacts do not imply that they do not exist. Therefore, ad-hoc tests are required to carefully evaluate how clean the output of an artifact-cleaning pipeline is. In Noury et al. (2016), we devised several methods for evaluating the

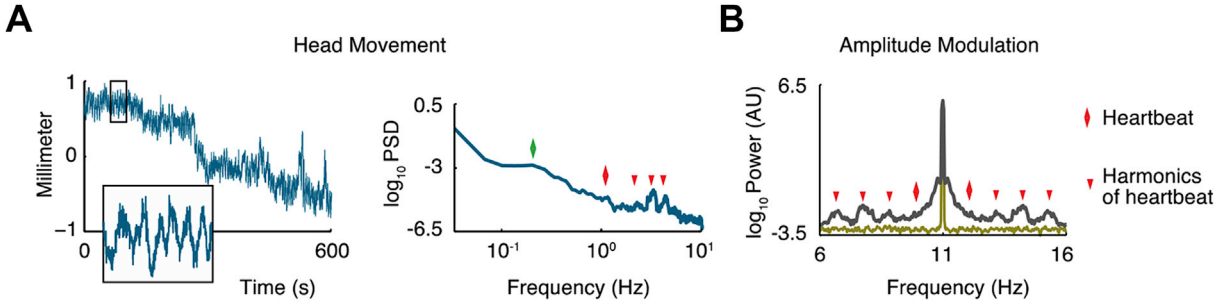

Fig. 2. (A) The left panel shows, 10 min of a healthy subject's head movement in the MEG system. Head movements contain both, rhythmic and non-rhythmic components. The inset shows 30 s of rhythmic head movements. The right panel shows the power spectrum of the same head-movement data. While non-rhythmic movements have a 1/f power spectrum, rhythmic movements lead to observable peaks in the power spectrum. In particular, heartbeats lead to rhythmic head movements. The red rhombus indicates the heartbeat frequency and red triangles indicate its harmonics. (B) Modulating the amplitude of an 11 Hz sinusoid with the normalized head movement signal yields a symmetric power spectrum. Heartbeat related peaks are symmetric around the 11 Hz peak. Also the 1/f head-movement component is reflected symmetrically around the 11 Hz peak.

output of different artifact-cleaning methods based on the artifact features explained above. Relevant to the present paper, for beamforming we suggested a cross-frequency spatial correlation test to check the spatial distribution of power of the beamformed data at different artifactual frequencies. The stimulation artifact leads to a non-physiological relation between the stimulation frequency and AM-related side-peak frequencies. We argued that, for artifact free beamformed data, there should be no significant relation between signals at these frequencies. Therefore, we suggested to test if the spatial distribution of power at the stimulation frequency is significantly correlated to the spatial distribution of power at side peak frequencies (i.e., stimulation frequency ± heartbeat and respiration related frequencies). In case of a significant correlation, the beamformed data contains residual artifacts at the stimulation and side peak frequencies (see Figure 8e in Noury et al., 2016).

4. Reply to Neuling et al

A recent paper (Neuling et al., 2017) claimed that the features of stimulation artifacts described in Noury et al. (2016) are merely due to technical problems of the stimulator or of the applied methods, and that these artifacts are largely absent in recordings of Neuling et al. Unfortunately, Neuling et al. (2017) made these claims without applying the critical artifact-detection tests that we suggested in Noury et al. (2016) to their data. In the following, we go through all sections of Neuling et al. (2017), and show that none of the raised concerns are correct or applicable to our results.

4.1. Reply to "the origin of the nonlinear artifacts"

There are four distinct points to discuss regarding this section of Neuling et al. (2017). First, the authors argue that the amplitude modulations (i.e. non-sinusoidal signals) reported in Noury et al. (2016) are attributable to technical issues, and that they have happened due to getting close to the technical limits of the stimulation device. Here we show that this is not the case.

If the stimulation device is used beyond its technical limits, the output current of the stimulator may be non-sinusoidal, i.e. show increased harmonics, and may become time-varying, which leads to artifacts at frequencies surrounding the stimulation frequency. We carefully ruled this out for all our experiments. First, we directly measured the stimulation current generated by our stimulation device and ensured that this current was sinusoidal. According to the Biot-Savart law (eq. (2)), direct evaluation of the stimulation current is the necessary and sufficient control analysis to rule out the influence of any technical issue related to the stimulation device. We showed that the stimulation current recorded during our experiments displayed neither any modulations locked to heartbeat or respiration in the time domain, nor side peaks at relevant frequencies in the frequency domain (Supplementary Fig. 1 of Noury et al., 2016). Moreover, by fit and removal of a single sinusoidal model, we showed that, at the stimulation and nearby frequencies, the output of our stimulation device was almost a pure sinusoid (Fig. 3A and B and Fig. 2 of Noury et al., 2016). Thus, in contrast to the claim of Neuling et al. (2017), we did not reach the technical limits of our stimulator and none of the results presented in our paper can be attributed to a dysfunction of the stimulation device.

It should be noted that our experimental procedures were carefully designed to prevent any technical problems caused by using the stimulator beyond its technical limits. We kept each stimulation electrode's resistance below 2.5 K Ohm (Noury et al., 2016). Consequently, the stimulator had to produce less than 5 V peak-to-peak sine waves to drive a stimulation current of 1 mA peak-to-peak. This is far below the dynamic range of the used stimulator (IZ2h stimulator, 24 V and 6 mA peak-to-peak output voltage and output current, respectively. This specification is wrongly reported in Neuling et al., 2017).

The second point is related to the detection of artifactual amplitude modulations in the raw data. Neuling et al. (2017) report that they have not been able to detect artifactual side peaks in about half of their subjects, and conclude that data from most of their subjects were not contaminated with non-linear artifacts. However, this claim is based on visual inspection of the raw signals' power spectra. As pointed out before (Noury et al., 2016) and above, such an inspection is prone to be affected by the strong power leakage of the main stimulation peak. Thus, one needs to first eliminate this leakage by fit and removal of a sine wave to be able to observe details of the power spectrum. Moreover, averaging over sensors blurs details of the spectra. Thus, for sensitive artifact detection, sensors should be separately investigated. We predict that after adding the above critical step and by following the analysis procedures suggested in Noury et al. (2016), artifactual side peaks will be observed in all the subjects. Importantly, even if after careful evaluation of the power spectrum, heartbeat and respiration-related side peaks are not present in some channels, a simple heartbeat or respiration-locked time-domain analysis of the artifact envelope must be applied, before concluding the absence of artifact modulations.

Third, Neuling et al. visually inspected averaged source level power spectra to evaluate residual artifacts in the beamformed data. As explained in the previous section, this test is not sufficiently sensitive. We also did not observe side peaks in our data at the source level (Fig. 4A). Therefore, in our original paper (Noury et al., 2016), we suggested and employed a more sensitive test, i.e. a cross-frequency spatial correlation analysis to investigate the presence of residual artifacts at the source level. Unfortunately, Neuling et al. (2017) did not perform this critical analysis.

Fourth, we would like to highlight an important difference between the phantom experiments of Neuling et al. and our experiments. In our experiments, we thoroughly recorded and analyzed the stimulation current to show that the stimulator successfully generated a constant amplitude sine wave. We feel that this is likely not the case for the phantom experiments of Neuling et al. In other words, we suspect that in their phantom experiments the stimulator failed to produce a constant amplitude sine wave. Although Neuling et al. did not measure the stimulation current, this can be inferred from the fact that, despite no movements of the melon phantom during the experiment (i.e. constant r' in eq. (2)), the power spectrum of the magnetic field at the sensor level (i.e. B in eq. (2)) shows more than one peak. Therefore, it can be inferred that the stimulation current (i.e. J in eq. (2)) was non-sinusoidal. This may have happened because of the 20 K Ohm electrode resistance of the employed tACS electrodes, which is much higher than the 2.5 K Ohm electrode resistance in our experiments. Such a high impedance may push the stimulator beyond its technical limits. In sum, the side peaks observed in the phantom results of Neuling et al. likely have a nature different from the side peaks presented in our paper: the former one is likely generated due to problems in the stimulator but the latter one is generated due to the subjects' head movements and body impedance changes.

4.2. Reply to "methodological concerns"

In this section, Neuling et al. (2017) argue that our equipment had increased the occurrence of the amplitude modulations and side peaks. First, they again point to the specifications of our electrical stimulator, which however, are wrongly reported (IZ2h stimulator, 24 V and 6 mA peak-to-peak output voltage and output current, respectively). In fact, the technical limits of our stimulator are higher than the limits of the stimulators that are commonly used in the field. Second, Neuling et al. discuss the potential role of the stimulation electrode size for artifact amplitude modulations, and speculate that higher current densities of smaller stimulation electrodes may contribute to the occurrence of side peaks. The results presented in Noury et al. (2016) show that this is not the case. The strengths of heartbeat- and respiration-locked modulations in experiments with small and large stimulation electrodes are very similar (compare topographies in Figs. 3, 4 and 6 of Noury et al., 2016). To

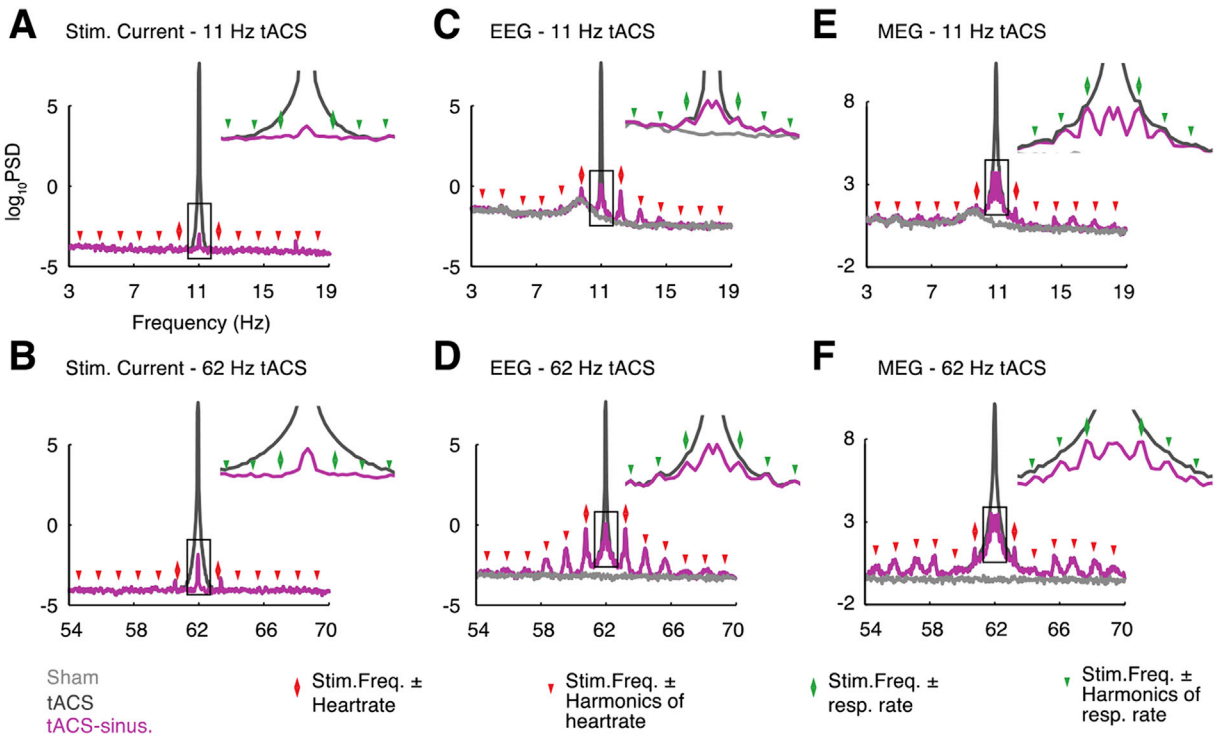

Fig. 3. Stimulation artifacts in the frequency domain for tACS experiment with large rubber stimulation electrodes. (A, B) High resolution power spectral density of the stimulation current (gray) around the stimulation frequency for 11 Hz and 62 Hz tACS. Smaller subplots show the power spectra zoomed into the stimulation frequency ±1 Hz. Importantly, subtracting a sinusoidal model from the stimulation current (magenta) removes almost all power of the stimulation current. This shows that the technical limits of the stimulator were not reached, and that the stimulator successfully generated a pure sinusoidal output current at the stimulation frequencies. (C, D) EEG power spectral density around the stimulation frequency during sham and tACS, with and without removal of a sinusoidal artifact model. (E, F) MEG power spectra for sham and tACS. Red and green rhombuses mark the stimulation frequency ± individual average heartbeat and respiration frequencies, respectively. Triangles mark harmonics of heartbeat and respiration frequencies. Peaks of EEG and MEG power are at the frequencies related to physiological processes. Subtracting the sinusoidal artifact uncovers details of the power spectrum for frequencies close to the stimulation frequency. In addition to side peaks, power spectra contain symmetric 1/f components, which likely reflect arrhythmic artifactual amplitude modulations. EEG and MEG data show channels CPz and MRT34, respectively.

further investigate this, we re-calculated the power spectra of the experiment with large stimulation electrodes (Fig. 3). In accordance with our previous results (Fig. 6 of Noury et al., 2016), high-resolution power spectra showed clear side peaks at heartbeat and respiration frequencies as well as at their harmonic frequencies, similar to the power spectra of the experiment with small stimulation electrodes. Notably, another recent tDCS study with large stimulation electrodes by an independent group of researchers (Marshall et al., 2015) also showed heartbeat-induced nonlinear stimulation artifacts at sensor and source levels. In sum, our results show amplitude modulations of tACS artifacts that are not attributable to the stimulator or to the size of the stimulation electrodes.

4.3. Reply to "the real tACS signal"

In this section, Neuling et al. repeat their assumption about the technical nature of amplitude modulations reported by us. We thoroughly discussed and falsified this assumption in previous sections (Fig. 3A and B and Fig. 2 of Noury et al., 2016). Nevertheless, it is still important to ask if, despite absence of a technical issue, neurons receive pure sinusoidal stimulation currents. In other words, if the stimulation current that is generated by the stimulator is not modulated, but the measured EEG voltages show modulations, what does this imply for the effect of tES on neurons? The effect on neurons depends only on the current that reaches them. In the present situation, the sum of stimulation currents flowing through the head is constant, i.e. equal to the stimulation current generated by the stimulator. But, the way that the current flows are distributed through the head may vary over time. For example, these variations could result from changes of the relative resistivity of the skull and the scalp, or of the relative resistivity of different parts of the scalp. Neurons experience such rhythmic and non-rhythmic modulations only if the spatial pattern of tES current flows varies in such a way that the currents that reach neurons are modulated. Our PCA analysis suggests that rhythmic changes in the spatial distribution of the stimulation currents indeed happen, but that these rhythmic variations are about 1000 times smaller than the average tES current (Figs. 3 and 4 of Noury et al., 2016). Thus, future simulation studies and invasive recordings are required to clarify to what extent rhythmic as well as non-rhythmic changes in current distribution reach neurons, and if neural responses are affected by these modulations (Ali et al., 2013; Fröhlich and McCormick, 2010; Huang et al., 2017; Opitz et al., 2016, 2015).

4.4. Reply to "regularization impedes beamforming performance"

In this section, Neuling et al. claim that the regularization factor (λ) used in our original paper (Noury et al., 2016) was not optimal. Here we show that this claim is wrong.

Fig. 2 of Neuling et al. (2017) shows the effect of λ on beamforming of tACS-MEG data and suggests using a λ close to zero for an optimum performance of the beamformer. The figure shows that the strength of residual artifacts, i.e. the peak at the stimulation frequency, monotonically increases with increasing λ. In this figure, the peak of the curve that is claimed to correspond to our method is bigger than the peak of the curve for a λ of 100% of the average MEG power. However, the average regularization factor that we used in Noury et al. (2016) was 2.5e-6% of the average MEG power (4e-7% STD across subjects). Thus, it follows that Neuling et al. did not correctly apply our method, but mistakenly assigned a λ bigger that 100% to our method. To correct this, we replicated their analysis and found that, as expected, the results for our method were indistinguishable from the results for a λ

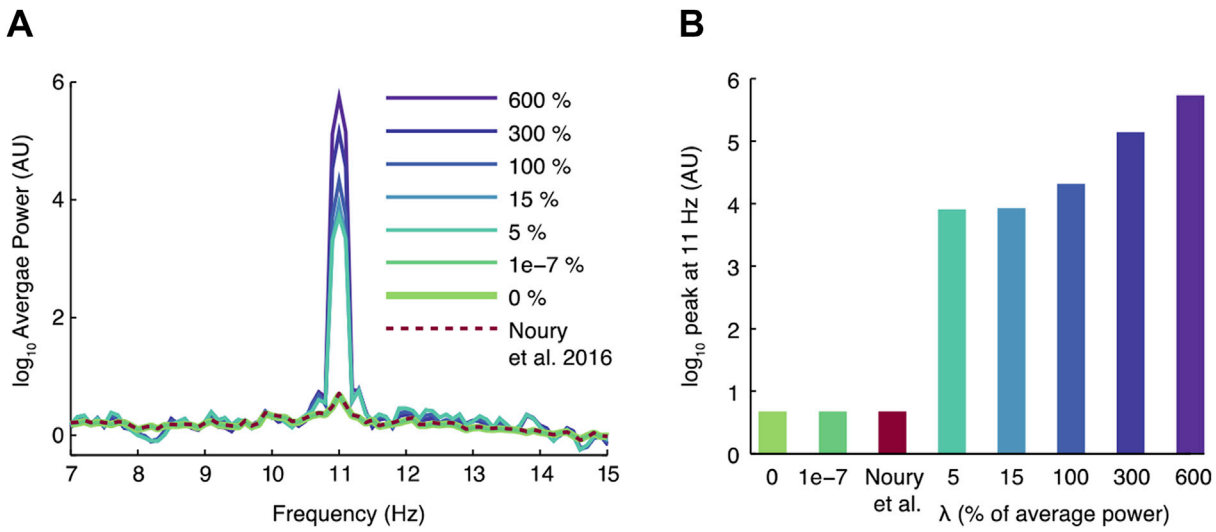

Fig. 4. Influence of the regularization factor (λ) on beamforming results. (A) Average source level power at the stimulation and nearby frequencies in one subject. Each curve corresponds to beamforming with a specific λ. Percentage is relative to the average MEG power during both sham and tACS. Darker curves have higher λ values. Note that some of the curves overlap with each other. The red dashed line corresponds to the λ used in Noury et al. (2016) (0.0000032% for this subject). (B) The average power at the stimulation frequency (11 Hz) is monotonically related to λ.

of zero or 7e-7% (Fig. 4).

Furthermore, related to this section of Neuling et al. (2017), it should be pointed out again that average power spectra, as provided by Neuling et al., are insufficient to conclude that source-level data is artifact free. As mentioned above, we also did not observe side peaks in the averaged source level power spectrum (Fig. 4A). In fact, in our paper we did not make any claims concerning the appearance of the source level power spectrum. However, difficulty in detecting artifactual side peaks in spectrum does not imply that the source level data is artifact free, especially because side peaks only represent the rhythmic part of artifact modulations. Therefore, we introduced a more sensitive test, which is evaluating the spatial distribution of power at different frequencies.

5. Discussion

Here, we discussed the physics underlying amplitude modulations of tES artifacts in EEG and MEG. These amplitude modulations are independent of the stimulation device or electrode size, and contain both non-rhythmic and rhythmic components. Both components should be removed from data before investigating brain activity. Rhythmic components generate landmarks in the data, and thus, provide opportunities to detect and track tES artifacts at different processing stages. We went through all points raised in Neuling et al. (2017) and showed that none of these points are correct or applicable to our results.

Stimulation artifacts in EEG and MEG are orders of magnitude larger than brain signals and have complex phase and amplitude features. However, it should be emphasized that it may still be possible to investigate brain activity during tES.

One approach is to employ new stimulation protocols that prevent tES artifacts in the frequency band of interest (Witkowski et al., 2016). The potential of such new stimulation protocols to manipulate brain activity should be thoroughly investigated (Chander et al., 2016). Another approach is to use established stimulation protocols, and employ artifact-removal pipelines to suppress stimulation artifacts strongly enough to be able to study brain activity in presence of residual artifacts. For this approach, it should be noted that all available artifact-cleaning pipelines, including beamforming, strongly attenuate tES artifacts. Therefore, it may be possible to devise specific measures or control experiments to check for the influence of residual artifacts. In the following, we first discuss why beamforming is unable to completely remove stimulation artifacts, and then provide ideas on how to account for residual artifacts and study brain activity in their presence (Table 1).

5.1. Beamforming as an artifact removal method

Although beamforming strongly reduces tES artifacts, it cannot completely remove them. Beamformed data contains residual artifacts (Marshall et al., 2015; Noury et al., 2016). We suggest that this is largely due to time varying (Noury et al., 2016) and phase-shifted (Noury and Siegel, 2017) artifact-leadfields. The former factor is a result of artifact amplitude modulations caused by head movements and body impedance changes. This leads to time varying pattern of tES artifacts at the sensor level. Therefore, a time invariant beamforming filter is not able to remove tES artifacts at all time points. The latter factor manifests itself in artifact phase deflections at the sensor level (Noury and Siegel, 2017). For both, EEG and MEG, tACS artifacts are not pure in-phase or anti-phase sinusoids, but have different phase shifts relative to the stimulation current, which is probably due to capacitive effects and time varying electromagnetic fields for EEG and MEG, respectively (see Noury and Siegel, 2017 for more information on phase features of tES artifacts). Theoretically, both factors can be modeled as artifact sources that are not 100% correlated with each other. Consequently, beamforming results contain residual artifacts that result from to the uncorrelated part of stimulation artifact (Mäkelä et al., 2017). In sum, beamforming results contain residual artifacts that should be accounted for. Next, we present some ideas how to cope with residual artifacts.

5.2. Artifact-sensitive control experiments

TES artifacts are easier observable at higher frequencies, for which MEG and EEG contain weaker physiological signals. Therefore, artifact-sensitive control experiments with high stimulation frequencies may be used to evaluate the strength and effects of residual artifacts. This is particularly useful when the tACS frequency of interest is in the alpha range or below, because at these low frequencies, strong brain signals mask the detectable features of tES artifacts, which in turn complicates estimating the strength of residual artifacts. Although tES may influence brain signals at any frequency, it seems unlikely that the very same physiological effects can be produced by stimulating at very different frequencies. Thus, one can compare the results and observed effects of

tES at the main stimulation frequency of interest with results and effects at tES at a higher artifact-sensitive control frequency to check if residual artifacts could drive the effects observed at the main tES frequency of interest.

5.3. Event related responses

Residual artifacts have little effect on event related potentials and fields. If tES waves are not time-locked to stimuli, and physiological processes do not become time-locked to either stimuli or tES waves, averaging brain responses time-locked to stimuli cancels out tES artifacts. In this situation, residual artifacts merely increase the noise level of trials. Therefore, the number of trials needed to obtain specific results will be larger than for experiments without tES.

5.4. Contrasting two populations under the same tES condition

If two signal populations contain the same amounts of tES artifacts, one can subtract their mean values from each other to cancel the effect of tES artifacts and to quantify the difference of brain activity between the two populations during tES. For example, these populations can be obtained from M/EEG signals at two different trial time-points, or from M/EEG signals of two different cognitive states. Importantly, both populations should be measured under the exact same tES condition. Furthermore, to ensure the same average residual artifacts for both populations, it needs to be ensured that the two populations have the same physiological states (heart rate, respiratory rate, body resistance etc.).

To give an example, one may ask if alpha power decrease or gamma power increase due to visual stimulation differs between sham and tES conditions. If there was no temporal relationship between tES waves and visual stimuli, and visual stimulation did not affect the physiological states of subjects, one may assume the same levels of residual tES artifacts before and after stimulation onset. Under this condition, the average power of these time points could be subtracted from each other, and the results from sham and tES conditions could be compared. However, it is important to note that during tES, the power at each time point contains residual tES artifacts. Therefore, non-linear contrasts like “percent change relative to baseline” cannot be compared between sham and stimulation conditions, simply because the baseline during tES contains residual artifacts, which is not the case for the sham condition. In other words, baseline power must be subtracted, but cannot be divided with.

5.5. Simulation

Another approach would be to quantitatively evaluate the performance of an available artifact-cleaning pipeline, and to check if the observed M/EEG effects could be attributed to residual artifacts. Currently, no phantom is available that reflects all features of tES artifacts. However, computer simulations could be used for such evaluations (Noury and Siegel, 2017). First, different features of tES artifacts can be estimated from sensor level recordings. Based on these features, simulated tES artifacts could be added to sham data. Then, the effect of artifact-cleaning of this simulated data could be compared to the results of artifact-cleaning of the real tES data to estimate if the observed effects could be accounted for by residual artifacts.

Acknowledgements

This work was supported by the Centre for Integrative Neuroscience (Deutsche Forschungsgemeinschaft, EXC 307). We thank Marcus Siems for providing the MEG head movement recordings, and Florian Sandhäger and Marcus Siems for their valuable comments on the manuscript.

References

Ali, M.M., Sellers, K.K., Fröhlich, F., 2013. Transcranial alternating current stimulation modulates large-scale cortical network activity by network resonance. J. Neurosci. 33, 11262–11275. https://doi.org/10.1523/JNEUROSCI.5867-12.2013.

Baillet, S., Mosher, J.C., Leahy, R.M., 2001. Electromagnetic brain mapping. IEEE Signal Process. Mag. 18, 14–30. https://doi.org/10.1109/79.962275.

Bergmann, T.O., Karabanov, A., Hartwigsen, G., Thielscher, A., Siebner, H.R., 2016. Combining non-invasive transcranial brain stimulation with neuroimaging and electrophysiology: current approaches and future perspectives. NeuroImage 140, 4–19. https://doi.org/10.1016/j.neuroimage.2016.02.012.

Brittain, J.-S., Probert-Smith, P., Aziz, T.Z., Brown, P., 2013. Tremor suppression by rhythmic transcranial current stimulation. Curr. Biol. CB 23, 436–440. https://doi.org/10.1016/j.cub.2013.01.068.

Chander, B.S., Witkowski, M., Braun, C., Robinson, S.E., Born, J., Cohen, L.G., Birbaumer, N., Soekadar, S.R., 2016. tACS phase locking of frontal midline theta oscillations disrupts working memory performance. Front. Cell. Neurosci. 120 https://doi.org/10.3389/fncel.2016.00120.

Dornhorst, A.C., Howard, P., Leathart, G.L., 1952. Respiratory variations in blood pressure. Circulation 6, 553–558. https://doi.org/10.1161/01.CIR.6.4.553.

Fertonani, A., Miniussi, C., 2016. Transcranial electrical stimulation: what we know and do not know about mechanisms. Neurosci. Rev. J. Bringing Neurobiol. Neurol. Psychiatry. https://doi.org/10.1177/1073858416631966.

Fisch, B., 1999. Fisch and Spehlmann's EEG Primer: Basic Principles of Digital and Analog EEG, 3e, 3 edition. Elsevier, Amsterdam; New York.

Fröhlich, F., McCormick, D.A., 2010. Endogenous electric fields may guide neocortical network activity. Neuron 67, 129–143. https://doi.org/10.1016/j.neuron.2010.06.005.

Helfrich, R.F., Schneider, T.R., Rach, S., Trautmann-Lengsfeld, S.A., Engel, A.K., Herrmann, C.S., 2014. Entrainment of brain oscillations by transcranial alternating current stimulation. Curr. Biol. 24, 333–339. https://doi.org/10.1016/j.cub.2013.12.041.

Huang, Y., Liu, A.A., Lafon, B., Friedman, D., Dayan, M., Wang, X., Bikson, M., Doyle, W.K., Devinsky, O., Parra, L.C., 2017. Measurements and models of electric fields in the in vivo human brain during transcranial electric stimulation. eLife 6, e18834. https://doi.org/10.7554/eLife.18834.

Kristiansen, N.K., Fleischer, J., Jensen, M.S., Andersen, K.S., Nygaard, H., 2005. Design and evaluation of a handheld impedance plethysmograph for measuring heart rate variability. Med. Biol. Eng. Comput. 43, 516–521.

Kuo, M.-F., Nitsche, M.A., 2012. Effects of transcranial electrical stimulation on cognition. Clin. EEG Neurosci. 43, 192–199. https://doi.org/10.1177/1550059412444975.

Lustenberger, C., Boyle, M.R., Alagapan, S., Mellin, J.M., Vaughn, B.V., Fröhlich, F., 2016. Feedback-controlled transcranial alternating current stimulation reveals a functional role of sleep spindles in motor memory consolidation. Curr. Biol. 26, 2127–2136. https://doi.org/10.1016/j.cub.2016.06.044.

Mäkelä, N., Sarvas, J., Ilmoniemi, R.J., 2017. Proceedings #17. A simple reason why beamformer may (not) remove the tACS-induced artifact in MEG. Brain Stimul. 10, e66–e67. https://doi.org/10.1016/j.brs.2017.04.110.

Marshall, T.R., Esterer, S., Herring, J.D., Bergmann, T.O., Jensen, O., 2015. On the relationship between cortical excitability and visual oscillatory responses - a concurrent tDCS-MEG study. NeuroImage. https://doi.org/10.1016/j.neuroimage.2015.09.069.

Michard, F., 2005. Changes in arterial pressure during mechanical ventilation. Anesthesiology 103, 419–428 quiz 449–445.

Neuling, T., Ruhnau, P., Fuscà, M., Demarchi, G., Herrmann, C.S., Weisz, N., 2015. Friends, not foes: magnetoencephalography as a tool to uncover brain dynamics during transcranial alternating current stimulation. NeuroImage 118, 406–413. https://doi.org/10.1016/j.neuroimage.2015.06.026.

Neuling, T., Ruhnau, P., Weisz, N., Herrmann, C.S., Demarchi, G., 2017. Faith and oscillations recovered: on analyzing EEG/MEG signals during tACS. NeuroImage 147, 960–963. https://doi.org/10.1016/j.neuroimage.2016.11.022.

Noury, N., Hipp, J.F., Siegel, M., 2016. Physiological processes non-linearly affect electrophysiological recordings during transcranial electric stimulation. NeuroImage 140, 99–109. https://doi.org/10.1016/j.neuroimage.2016.03.065.

Noury, N., Siegel, M., 2017. Phase properties of transcranial electrical stimulation artifacts in electrophysiological recordings. NeuroImage 158, 406–416. https://doi.org/10.1016/j.neuroimage.2017.07.010.

Nyboer, J., Kreider, M.M., Hannapel, L., 1950. Electrical impedance plethysmography a physical and physiologic approach to peripheral vascular study. Circulation 2, 811–821. https://doi.org/10.1161/01.CIR.2.6.811.

Oostenveld, R., Fries, P., Maris, E., Schoffelen, J.-M., 2011. FieldTrip: open source software for advanced analysis of MEG, EEG, and invasive electrophysiological data. Comput. Intell. Neurosci. 2011, 156869. https://doi.org/10.1155/2011/156869.

Opitz, A., Falchier, A., Yan, C.-G., Yeagle, E.M., Linn, G.S., Megevand, P., Thielscher, A., Deborah, A.R., Milham, M.P., Mehta, A.D., Schroeder, C.E., 2016. Spatiotemporal structure of intracranial electric fields induced by transcranial electric stimulation in humans and nonhuman primates. Sci. Rep. 6, 31236. https://doi.org/10.1038/srep31236.

Opitz, A., Paulus, W., Will, S., Antunes, A., Thielscher, A., 2015. Determinants of the electric field during transcranial direct current stimulation. NeuroImage 109, 140–150. https://doi.org/10.1016/j.neuroimage.2015.01.033.

Oppenheim, A.V., Schafer, R.W., 2009. Discrete-time Signal Processing, 3 edition. Pearson, Upper Saddle River.

Pinheiro, E., Postolache, O., Girão, P., 2010. Theory and developments in an unobtrusive cardiovascular system representation: ballistocardiography. Open Biomed. Eng. J. 4, 201–216. https://doi.org/10.2174/1874120701004010201.

Romei, V., Thut, G., Silvanto, J., 2016. Information-based approaches of noninvasive transcranial brain stimulation. Trends Neurosci. 39, 782–795. https://doi.org/10.1016/j.tins.2016.09.001.

Soekadar, S.R., Witkowski, M., Cossio, E.G., Birbaumer, N., Robinson, S.E., Cohen, L.G., 2013. In vivo assessment of human brain oscillations during application of transcranial electric currents. Nat. Commun. 4 https://doi.org/10.1038/ncomms3032.

Stolk, A., Todorovic, A., Schoffelen, J.-M., Oostenveld, R., 2013. Online and offline tools for head movement compensation in MEG. NeuroImage 68, 39–48. https://doi.org/10.1016/j.neuroimage.2012.11.047.

Thut, G., Bergmann, T.O., Fröhlich, F., Soekadar, S.R., Brittain, J.-S., Valero-Cabré, A., Sack, A.T., Miniussi, C., Antal, A., Siebner, H.R., Ziemann, U., Herrmann, C.S., 2017. Guiding transcranial brain stimulation by EEG/MEG to interact with ongoing brain activity and associated functions: a position paper. Clin. Neurophysiol. 128, 843–857. https://doi.org/10.1016/j.clinph.2017.01.003.

Van Veen, B.D., van Drongelen, W., Yuchtman, M., Suzuki, A., 1997. Localization of brain electrical activity via linearly constrained minimum variance spatial filtering. IEEE Trans. Biomed. Eng. 44, 867–880. https://doi.org/10.1109/10.623056.

Voss, U., Holzmann, R., Hobson, A., Paulus, W., Koppehele-Gossel, J., Klimke, A., Nitsche, M.A., 2014. Induction of self awareness in dreams through frontal low current stimulation of gamma activity. Nat. Neurosci. https://doi.org/10.1038/nn.3719 advance online publication.

Witkowski, M., Garcia-Cossio, E., Chander, B.S., Braun, C., Birbaumer, N., Robinson, S.E., Soekadar, S.R., 2016. Mapping entrained brain oscillations during transcranial alternating current stimulation (tACS). NeuroImage. Transcranial Electr. Stimul. (tES) Neuroimaging 140, 89–98. https://doi.org/10.1016/j.neuroimage.2015.10.024.